HHS Public Access

Author manuscript

Oncogene. Author manuscript; available in PMC 2016 December 23.

Published in final edited form as:

Oncogene. 2016 June 23; 35(25): 3282–3292. doi:10.1038/onc.2015.389.

NFATc1 Promotes Prostate Tumorigenesis and Overcomes PTEN Loss-Induced Senescence

Kalyan R. Manda[1], **Piyush Tripathi**[2], **Andy C. Hsi**[3], **Jie Ning**[1,3], **Marianna B. Ruzinova**[2], **Helen Liapis**[2], **Matthew Bailey**[3], **Hong Zhang**[4], **Christopher A. Maher**[1,3,5], **Peter A. Humphrey**[6], **Gerald L. Andriole**[5,7], **Li Ding**[1,3,5], **Zongbing You**[8], and **Feng Chen**[1,5,9,*]

[1]Department of Medicine, Washington University, St. Louis, MO, 63110, USA

[2]Department of Pathology and Immunology, Washington University, St. Louis, MO, 63110, USA

[3]The Genome Institute, Washington University, St. Louis, MO, 63110, USA

[4]Department of Cell and Developmental Biology, University of Massachusetts Medical School, Worcester, MA, 01655, USA

[5]Siteman Cancer Center, Washington University, St. Louis, MO, 63110, USA

[7]Department of Surgery, Washington University, St. Louis, MO, 63110, USA

[8]Department of Structural and Cellular Biology, Tulane University, New Orleans, LA, 70112, USA

[9]Department of Cell Biology and Physiology, Washington University, St. Louis, MO, 63110, USA

Abstract

Despite recent insights into prostate cancer (PCa)-associated genetic changes, full understanding of prostate tumorigenesis remains elusive due to complexity of interactions among various cell types and soluble factors present in prostate tissue. We found upregulation of Nuclear Factor of Activated T Cells c1 (NFATc1) in human PCa and cultured PCa cells, but not in normal prostates and non-tumorigenic prostate cells. To understand the role of NFATc1 in prostate tumorigenesis in situ, we temporally and spatially controlled the activation of NFATc1 in mouse prostate and showed that such activation resulted in prostatic adenocarcinoma with features similar to those seen in human PCa. Our results indicate that the activation of a single transcription factor, NFATc1 in prostatic luminal epithelium to PCa can affect expression of diverse factors in both cells harboring the genetic changes and in neighboring cells through microenvironmental alterations. In addition to the activation of oncogenes c-MYC and STAT3 in tumor cells, a number of cytokines and growth factors, such as IL1β, IL6, and SPP1 (Osteopontin, a key biomarker for PCa), were upregulated in NFATc1-induced PCa, establishing a tumorigenic microenvironment involving both NFATc1 positive and negative cells for prostate tumorigenesis. To further characterize interactions between genes involved in prostate tumorigenesis, we generated mice with both NFATc1

*Corresponding Author: Feng Chen, Department of Medicine, Campus Box 8126, Washington University School of Medicine, St. Louis, MO 63110, USA. Phone: (314) 362-3162; Fax: (314) 362-8237; fchen@dom.wustl.edu.

[6]Current Address: Department of Pathology, Yale University, New Haven, CT, 06520, USA.

The authors declare no conflict of interest.

activation and Pten inactivation in prostate. We showed that NFATc1 activation led to acceleration of Pten-null–driven prostate tumorigenesis by overcoming the PTEN loss–induced cellular senescence through inhibition of p21 activation. This study provides direct in vivo evidence of an oncogenic role of NFATc1 in prostate tumorigenesis and reveals multiple functions of NFATc1 in activating oncogenes, in inducing proinflammatory cytokines, in oncogene addiction, and in overcoming cellular senescence, which suggests calcineurin-NFAT signaling as a potential target in preventing PCa.

Keywords

NFAT; *Prostate Cancer*; PTEN; *Senescence*; *Microenvironment*

Introduction

Recent discoveries in prostate cancer (PCa) research have highlighted a number of key genetic alterations in driving prostate tumorigenesis. Despite these advances, the progression from the initial genetic changes to clinically significant PCa is still not fully understood.[1] Furthermore, the interactions of various genes involved in pathogenesis of prostate cancer needs to be further investigated.

The NFAT (Nuclear Factor of Activated T cells) family of transcription factors are important for many diverse cellular processes including T cell activation, cardiac valve development, and osmotic stress response.[2, 3] The NFAT family includes four NFATc proteins (c1–c4) and NFAT5. The NFATc proteins reside in the cytoplasm in quiescent cells. The Ca^{2+}-dependent serine/threonine phosphatase Calcineurin, when activated by an increase in intracellular Ca^{2+}, dephosphorylates the NFATc proteins and exposes their concealed nuclear localization signals, causing them to translocate from cytoplasm to the nucleus.[2, 3] Once in the nucleus, NFATc proteins complex with cell-type specific cofactors to control the transcription of target genes. Phosphorylation of NFATc by GSK3β and other kinases promotes nuclear export of these proteins.

NFATc1 activation was shown to induce transformation and colony formation in 3T3-L1 preadipocytes.[4] Elevated or ectopic NFATc1 activation has also been observed in multiple types of human tumors.[3, 5] NFAT proteins have also been found to regulate proliferation and growth of multiple human tumor cells, including PCa cells.[3, 6, 7] NFATc1 has been shown to regulate prostate specific membrane antigen and genes involved in osteoclastogenesis induced by PCa cells.[8–10] Besides growth and proliferation, components of the calcineurin-NFAT signaling pathway, including NFATc1, have also been linked to cell migration, tumor invasion, and metastasis in human cancers.[3, 11–15] NFATc1 effects are not always pro-growth and some NFATc genes may act as tumor suppressors.[3, 16] NFATc1 activation can lead to cell loss and fibrosis in some contexts.[3, 17] Thus, biological consequences of NFAT activation in different tissues may be very different and the molecular mechanism by which Calcineurin-NFAT affects PCa *in situ* is hard to predict and needs to be directly studied.

In this study, we generated a murine model where NFATc1 activation can be induced in prostate epithelium. The activation of NFATc1 results in prostatic intraepithelial neoplasia

(PIN) which progresses to prostate adenocarcinoma. We further demonstrated that NFATc1 activation establishes a promitogenic microenvironment with upregulation of proinflammatory cytokines and growth factors. We have also shown that NFATc1 and the PTEN-AKT pathway act synergistically in promoting PCa since NFATc1 activation overcomes the PTEN-loss-induced cellular senescence. This study provides direct *in vivo* evidence of an oncogenic role of NFAT in PCa and offers insights into multi-faceted progression from a defined transcriptional change in prostatic epithelia to prostate tumorigenesis involving both cell autonomous changes in oncogenic protein expression and the effects of secreted factors in the microenvironment.

Results

NFATc1 expression is detected in human PCa specimens and PCa cells but is absent in non-neoplastic human prostates and non-tumorigenic prostatic cells

NFATc1 expression has been previously reported in human PCa specimens.[18–20] Using human normal prostate and PCa specimens from Biomax (MD, USA) and from archived patient specimens, we found NFATc1^{+} cells in the neoplastic epithelium in 18 (~30%) of the adenocarcinoma specimens (N=57) with Gleason scores ranging from 5–9, but not in the epithelium of non-neoplastic prostates (N=30) (Fig. 1A–C). NFATc1^{+} cells were also present in the tumor stroma. In addition, we have found NFATc1 expression in the human malignant PC3, LNCaP, and DU145 cells, but not in the non-tumorigenic RWPE1 cells (Fig. 1D–G). These results are consistent with previous findings that NFATc1 expression is associated with the initiation, progression, and probably even the metastasis of the various cancers,[3] including PCa.[7, 20]

Inducible NFATc1 activation in prostatic epithelium causes PIN and prostatic adenocarcinoma

To investigate the potential role of NFAT signaling in PCa, we created a mouse model for inducible NFATc1 activation in cells targeted by the *PBCre4* (*PCre*) transgene[21] with known expression in the prostatic epithelium. In this system, Cre expression induces the removal of the transcriptional stop cassette in a *ROSA*^{rtTA} (*RT*) allele[22] and the production of rtTA (reverse *tetracycline*-controlled transactivator). In the presence of doxycycline (Dox), the Dox-rtTA complex binds to the *TetO* sequence of the *TetO-NFATc1*^{Nuc} (*TN*) transgene[23] to induce the transcription of *NFATc1*^{Nuc} (an activated form of NFATc1)(Fig. 2A). We refer to mice carrying all three alleles (*PCre*, *RT*, *TN*) as mutants. Their littermates missing any of these alleles cannot have NFATc1 activation, even in the presence of Dox, and thus are regarded as controls. *NFATc1*^{Nuc} transcripts were detected in Dox-treated mutants, but not in similarly treated controls (Fig. 2B).

We treated control-mutant pairs (n=23) with Dox from weaning (P21-postnatal day 21) for variable lengths of time. We found a dramatic expansion of the prostate lobes in mutants treated for 14 weeks (Fig. 2C–D). Although mutants treated for 6 weeks (n=6) did not show dramatic outward changes, histological analyses showed that they already had PIN recognized by proliferation and stratification of epithelial cells (Fig. 2E–F). 96% (22/23) of the mutants with NFATc1 activation for 14 weeks had PCa in the dorsolateral and ventral

prostate lobes (Fig. 2G–H) whereas all controls had normal epithelium. The majority of human PCa is found in the peripheral zone that is most similar to the mouse dorsolateral lobes. About half of the mutants also developed PCa in the anterior prostate. The remaining half either had PIN or failed to develop any significant neoplastic changes in the anterior prostate. The murine PCa showed an acinar growth pattern, similar to those seen in human prostatic acinar adenocarcinoma.

NFATc1-induced PCa has cellular composition resembling human prostatic adenocarcinoma

Normal prostate gland has a Cytokeratin 5 $(CK5)^+$ and $p63^+$ basal epithelial cell layer, a Cytokeratin 8 $(CK8)^+$ luminal epithelial cell layer with Androgen Receptor (AR) expression, a small number of Synaptophysin $(SYNAP)^+$ neuroendocrine cells, and the surrounding myofibroblast cells that are α-Smooth muscle actin $(SMA)^+$ (Fig. 3A, C, E, G, and I). In mutants with NFATc1 activation for 14 weeks starting from P21, tumor expansion primarily came from $CK8^+/AR^+$ luminal epithelial cells (Fig. 3B, D, F, H, J), a situation similar to the most common type of human PCa. $CK5^+$ basal cells and $SYNAP^+$ neuroendocrine cells were mostly absent from tumor proper and were found in adjacent glands that are either benign or apparently in transition to neoplasia. SMA^+ fibromuscular layers surrounding the prostatic glands lost continuity or were absent in many areas in these mutants, likely as the result of invasion of $CK8^+$ cells into the stroma (Fig. 3J).

Active proliferation of NFATc1$^-$ cells appears to result from a promitogenic microenvironment

In addition to a high percentage of $NFATc1^+$ cells (49.5±4.40%) in the PCa being $PCNA^+$ (proliferating), many neighboring $NFATc1^-$ cells (15.8±2.57%%) were also $PCNA^+$ (Fig. 4A–C). Interestingly, while 56.6±7.45% $NFATc1^+$ cells were expressing c-MYC, 32.4±4.0% $NFATc1^-$ cells also had c-MYC expression in the PCa (Fig. 4D–F). Furthermore, 59.1±8.31% $NFATc1^+$ and 16.63±2.11% $NFATc1^-$ cells had nuclear phospho-STAT3 (pSTAT3) (Fig. 4G–I). STAT3 activation in $NFATc1^-$ cells cannot directly result from NFAT transcriptional regulation. Instead, such changes may be due to microenvironmental alterations. These observations are consistent with previous findings that cultured cells expressing an active NFATc1 secrete unidentified and heat labile factors to promote the proliferation of other cells that are $NFATc1^-$ [4, 24]. Immunoblotting of lysates from normal prostates and NFATc1-induced PCa showed that the level of pSTAT3 was greatly increased in NFATc1-induced PCa, though total STAT3 level was unchanged (Fig. 4J).

Increased expression of proinflammatory cytokines and other factors in NFATc1-induced PCa

We selected a number of cytokines and secreted factors for further analyses in the PCa based on our previous findings[25] and other studies linking them to NFAT[3] and/or PCa.[26] By RT-PCR, we showed that NFATc1 activation was accompanied by increased levels of transcripts from Spp1, Saa3, IL6, IL1β, IL1α, Ccl3, Lcn2, and others (Fig. 5A), some of which were implicated in promoting PCa progression.[27] By immunofluorescent staining, we showed significantly elevated levels of secreted cytokines, such as Spp1 and its receptor CD44, IL6, and IL1β, in the PCa (Fig. 5B–I). Spp1 has been reported as an important diagnostic and

prognostic biomarker for PCa and some of the NFATc1 oncogenic effects may be channeled through the upregulation of Spp1.[27, 28]

Tumor progression and survival depend on activation of NFATc1 but not on T cell functions

To directly test the essential role of NFATc1 activation in tumorigenesis and to examine the involvement of lymphocytes in establishing the tumorigenic microenvironment, we studied the ability of the cells with NFATc1 activation to initiate tumorigenesis in nude mice with absence of T cells. We derived tumor cells from NFATc1-induced murine PCa and showed that about 70% of these cells expressed NFATc1 and the HA (human influenza hemagglutinin) tag fused to the C-terminus of NFATc1 (Fig. 6A), but no $CD45^+$ cells were present (data not shown). These cells were injected to the rear flanks of the nude mice. Tumor growth was detected as early as 4 weeks after the injection in the Dox-treated (with NFATc1 activation), but not in the untreated (without NFATc1 activation), recipient mice (Fig. 6B–D). To further test the dependency of tumor growth and progression on NFATc1 activation, we stopped Dox treatment in a subgroup of these mice. Existing tumors started to shrink within days after Dox withdrawal (Fig. 6D). This trend was reversed when NFATc1 activation was restored with Dox treatment (Fig. 6D), indicating a continuous dependency of the PCa on NFATc1 activation, similar to that seen in cases of oncogene addiction.[29–31] Histopathological analyses of tumors revealed that these allografts contained carcinoma with a more solid growth pattern but showed cytological features similar to those seen in original tumors (Fig. 6E), including the presence of a large number of $NFATc1^+$/$E\text{-}Cad^+$ cells (Fig. 6F) and STAT3 activation in both $NFATc1^+$ and $NFATc1^-$ cells that intermingled within the tumor proper (Fig. 6G). Since inflammatory cytokines, such as IL6, are similarly upregulated in the grafts (Fig. 6H), the establishment of the inflammatory tumorigenic microenvironment thus appears independent of T cells, but likely dependent on the tumor cells, local tissue resident cells, and other immune cells in this model.

NFAT signaling can overcome androgen deprivation to drive PCa progression

Androgens are critical both for development and function of the prostate gland and for the survival and proliferation of the epithelial cells.[32] In order to determine if NFATc1-induced PCa would respond to hormone deprivation therapy, we analyzed prostates from 18-week-old mutant mice with NFATc1 activation since weaning and were either castrated or mock-castrated at 14 weeks of age. PCa samples from castrated and mock-castrated mutants are similar in tumor size and histopathological features (Fig. 7A–B). However, the distinct nuclear AR staining seen in the prostate of non-castrated mice was replaced by a more diffused and weaker expression pattern in castrated mice, indicating that castration had effectively reduced AR signaling in prostatic cells (Fig. 7C–D). Tumors from both mock-castrated and castrated mice had significant number of $PCNA^+$ proliferating cells, indicating that androgen deprivation had little or no effect on NFATc1-induced PCa and their proliferation (Fig. 7E–F).

NFATc1 activation synergizes with the PI3K-AKT pathway to promote PCa progression

Pten is one of the most frequently mutated tumor suppressors in PCa.[33, 34] To understand if and how the NFAT and PI3K-AKT pathways interact in PCa, we generated mice with both

Pten deficiency and NFATc1 activation in prostatic epithelia. At 10 weeks of age, most *PCre/+;Pten*$^{fl/fl}$ mice with only PTEN deficiency in the prostate epithelium showed enlarged anterior prostates, whereas control and *PCre/+;RT/+;TN/+* mice with only NFATc1 activation starting from P21 in prostatic epithelium had no visible tumors. Interestingly, all double mutants (*PCre/+;RT/+;TN/+;Pten*$^{fl/fl}$) with both PTEN deficiency and NFATc1 activation developed significantly larger tumors in all prostate lobes when compared to mice of the same age with either Pten deficiency or NFATc1 activation alone (Fig. 8A–D). The average prostate weight in double mutants (6026.24±1946.85 mg) was increased 17.41-fold when compared to the controls (346.85±36.66 mg), 15.45-fold when compared to mice with NFAT activation alone (390.28±73.16 mg), 7.35-fold when compared to *Pten* null mice (819.14±139.4 mg, Fig. 8Q). Histopathological analyses revealed that *Pten* null mice and mice with NFATc1 activation alone had PIN at this time, whereas double mutants already had poorly differentiated prostatic adenocarcinoma (Fig. 8E–H). While levels of pAKT were low in prostates from controls and mice with only NFATc1 activation, increased expression of pAKT was apparent in *PCre/+;Pten*$^{fl/fl}$ and *PCre/+;RT/+;TN/+;Pten*$^{fl/fl}$ samples, indicating that the PI3K-AKT pathway was activated in prostates with PTEN loss (Fig. 8I–L). SMA staining revealed intact myofibroblast layers in the prostates from single mutants but widespread disintegration of the SMA layer in double mutants, consistent with invasion of the epithelial cells into the stroma (Fig. 8M–P). These findings reveal that NFATc1 activation synergizes with PTEN-AKT pathway for PCa initiation and progression.

NFATc1 activation overcomes PTEN-loss-induced cellular senescence through down regulation of cell cycle inhibitors

It has been shown that senescence plays a tumor-suppressive role in PTEN-deficient cells, explaining the long tumor latency in murine models with PTEN-deficient prostate.[34] The earlier onset and faster progression of PCa in double mutants suggest that NFATc1 activation may allow the tumor cells to avoid the PTEN-loss-induced cellular senescence, resulting in accelerated tumor growth. Therefore, we examined markers of proliferation and senescence in prostates from (*PCre/+;Pten*$^{fl/fl}$), (*PCre/+;RT/+;TN/+*), and (*PCre/+;RT/+;TN/+; Pten*$^{fl/fl}$) mice. The *PCre/+;RT/+;TN/+;Pten*$^{fl/fl}$ tumors had significantly higher levels of proliferation (68.87±18.37%) than the *PCre/+;Pten*$^{fl/fl}$ (24.16±6.76%), and *PCre/+;RT/+;TN/+* (33.46±3.72%) tumors, as assessed by PCNA staining (Fig. 9A–D, M). Furthermore, there was a marked decrease in the expression of the senescence marker p21 in *PCre/+;RT/+;TN/+;Pten*$^{fl/fl}$ samples when compared with the *PCre/+;Pten*$^{fl/fl}$ mice (Fig. 9E–H, arrowhead and inset). p21 staining was predominantly nuclear in *PCre/+;Pten*$^{fl/fl}$ prostates (63.6±7.95%). In contrast, nuclear p21 expression was absent in *PCre/+;RT/+;TN/+;Pten*$^{fl/fl}$ (4.2±1.30%) prostates, where cytoplasmic p21 was occasionally observed (Fig. 9N). While nuclear p21 is considered as tumor suppressors, cytoplasmic p21 may have anti-apoptotic roles and enhance cell survival.[35, 36] To further confirm that NFATc1 activation overcomes PTEN-loss-induced cellular senescence, we stained for senescence-associated β-galactosidase (SA-β-gal) activity in the prostates. Control and *PCre/+;RT/+;TN/+* prostates showed very few senescent cells, 1% *and* 6.66±0.5%, respectively. In contrast, 65.6±8.7% cells within the *PCre/+;Pten*$^{fl/fl}$ prostates were SA-β-gal^{+}. Such SA-β-gal^{+} cells in the *PCre/+;RT/+;TN/+;Pten*$^{fl/fl}$ prostates were dramatically reduced to 5.8±1.3% (Fig. 9I–L, O), supporting the

hypotheses that NFATc1 overcomes Pten-induced cellular senescence by down regulating cell cycle inhibitors.

Discussion

In this study, we have shown higher levels of NFATc1 expression in human PCa specimens and in PCa cell lines when compared to non-neoplastic prostates and non-tumorigenic prostatic cells (Fig. 1), consistent with a recent reports of NFATc1 expression in human PCa specimens.[7] By using a mouse model for prostate-specific and Dox-inducible NFATc1 activation, we have demonstrated that NFATc1 activation in luminal prostatic epithelial cells causes prostate adenocarcinoma with histopathological features similar to the most common type of human prostate adenocarcinoma (Figures 2 and 3). We further showed that NFATc1 activation promotes PCa by upregulating key oncogenic proteins and by establishing a promitogenic and proinflammatory microenvironment (Figures 4 and 5). We have further demonstrated that NFATc1 activation can overcome PTEN-loss-induced cellular senescence, greatly accelerate PCa progression associated with PTEN deficiency (Figures 8 and 9). Our results from the mouse model provide the direct *in vivo* evidence that NFATc1 can function as a robust oncogene in prostate tumorigenesis.

The upregulation of c-MYC and activation of pSTAT3 in both NFATc1$^+$ and NFATc1$^-$ cells cannot be the sole direct results of transcriptional regulation by NFATc1. Instead, in addition to the apparent cell autonomous effects of NFATc1 activation in the regulation of c-MYC, part of the impact from NFATc1 activation appears to go through the production of one or more secreted factors whose existence was first suggested by Neal *et al.* when studying the effects of NFATc1 activation in cultured 3T3-L1 cells.[4] We have demonstrated the increased expression of multiple cytokines (including IL6, IL1, SPP1 etc., Fig. 5) that have the potential to initiate, or at least contribute to, a proinflammatory and promitogenic microenvironment. Multiple recent studies have collectively indicated that SPP1 is one of the four key signatures genes correlated with PCa progression and prognosis.[27] Direct transcriptional regulation of SPP1 by NFAT has been reported in arteries,[28] consistent with our finding of increased SPP1 levels in mice with NFATc1 activation. Elevated IL6 levels are found in human PCa specimens and even in serum of patients with untreated metastatic or castration-resistant prostate cancer (CRPC) where IL6 levels correlate negatively with tumor survival and response to chemotherapy.[37, 38] NFATc1 activation-induced upregulation of IL6 and other proinflammatory cytokines (Figures 4 and 6) can activate the JAK-STAT pathway in both NFATc1$^+$ and NFATc1$^-$ cells, as revealed by our data of STAT3 activation in the PCa (Fig. 4), leading to promitogenic effects, including the upregulation of c-MYC that is known to be a target of STAT3 regulation.[39–41] Clinical trials with anti-IL6 antibody therapy has not yet demonstrated beneficial effects in advanced PCa.[37, 38] Although there may be many explanations, the wide range of cytokine activation in the microenvironment, as seen in the NFATc1-induced PCa, predicts that monotherapy targeting any one of them would not be particularly effective.

As our data support the notion that NFATc1 can be a potent oncogene for PCa through its cell autonomous and non-autonomous effects, we went a step further to ask if and how NFATc1 activation may interact with other commonly occurring prostate cancer mutations.

PTEN is an important tumor suppressor and is frequently mutated in PCa.[42] By introducing NFATc1 activation to mice deficient for *Pten*, we have showed synergistic effects of NFATc1 activation and Pten inactivation/Akt activation, as evident by the earlier onset and greater aggressiveness of the PCa in the double mutants. The mechanistic base of such synergism is likely that the introduction of the NFATc1 activation confers the cells the ability to overcome PTEN-loss-induced cellular senescence (Figures 8 and 9). Although the detailed mechanism for the anti-senescence effects of NFATc1 activation requires further investigation, it is possible that NFATc1-Interleukins-JAK-STAT3 axis upregulates the expression of SKP2, which in turn, suppresses the expression of p21. This hypothesis is consistent with the observations that SKP2 can be induced by activated STAT3 and that SKP2 negatively regulates p21.[43, 44] Regardless of the specific pathways affected, the anti-senescence effects of NFATc1 activation can conceivably enhance the tumorigenic effects of mutations in other genes associated with prostate tumorigenesis.

We have so far not been able to find evidence of metastasis of the NFATc1-induced PCa in mice with NFATc1 activation in the prostate for as long as 5 months. Although it is possible that metastasis may occur if the PCa progresses further, this cannot be determined in the current system we use due to lesions in the ears of the mutant mice that result in the euthanasia of the mice by animal study protocol. The exact cause of these lesions is unknown but appears to be related to ectopic expression of the *PCre* transgene used. As such, the question of potential metastasis in older mice will be investigated when more specific Cre drivers become available.

Although we have shown that NFATc1 activation drives PCa initiation and progression, we do not expect that genetic mutations of the NFATc1 gene to be a major mechanism for NFATc1 activation. This is because that the ligand-independent activation of NFATc1 requires blocking multiple phosphorylation sites. Random mutations within NFATc1 will most likely inactivate but not activate the protein.[3] Instead, the activation of NFATc1 is likely a result of mutations in genes whose protein products act upstream of NFATc1. One of such upstream factors may be TRPV6 that has been linked to human PCa and thought to enhance proliferation and apoptotic resistance through the upregulation of the calcium-Calcineurin-NFAT pathway.[6] Since NFATc1 activation in the prostate has pleiotropic effects on the cells expressing it and on the neighboring cells through alterations in multiple signaling factors in the microenvironment, inhibiting NFATc1 activation could be more effective than targeting one or more of the downstream pathways and factors in treating cancers with NFATc1 activation. The recent findings that Calcineurin-NFAT inhibitors suppressed proliferation, migration, and invasion of cultured prostate cancer cells[7], as well as that Silibinin suppressed the PCa cells-induced osteoclastogenesis partially through the inhibition of NFATc1[10] are encouraging and in broad agreement with data presented in this report. Our *in vivo* data on oncogene addiction and the ability of NFATc1 activation to continue to drive PCa progression after castration further suggest an oncogenic role of NFAT in CRPC and the potential benefits in inhibiting NFAT pathway in fighting PCa.

Materials and Methods

Mouse (Mus musculus) strains and Dox treatment

All animal studies were approved by the Washington University Animal Studies Committee and have been conducted according to relevant NIH guidelines. The *PBCre4-Cre* (*PCre/+*), *ROSA*^{rtTA} (*RT*), *TetO-NFATc1*^{Nuc} (*TN*) strains and the genotyping methods were described previously.[17, 21–23] For *NFATc1*^{Nuc}, the substitution of the serines targeted for phosphorylation and dephosphorylation with alanines renders the modified NFATc1 proteins constitutively nuclear and active. For studying interactions between NFAT and PTEN, *PCre* mice were crossed with *Pten*$^{fl/fl}$ mice (The Jackson Laboratory, Bar Harbor, ME, USA) to generate *PCre/+;Pten*$^{fl/+}$ males. These *PCre/+;Pten*$^{fl/+}$ mice were then crossed to *RT/RT;TN/+;Pten*$^{fl/fl}$ mice to generate controls and *PCre/+;RT/+;TN/+;Pten*$^{fl/fl}$ mutants. Dox was given through drinking water provided *ad libitum* at 2 mg/ml, starting at P21. Drastic morphological differences makes blinding of specimens from different genotype groups ineffective in this study.

Statistical Analyses

We use all available specimens that meet the quality standards. All quantitative data are presented as mean ± s.d. Two-tailed t-tests were performed between groups and $p < 0.05$ is considered significant.

Human Prostate Specimens

Formalin-fixed paraffin-embedded human specimens were obtained from the archives of prostate biopsies in the Department of Pathology and Immunology at Washington University School of Medicine. The human studies protocol was approved by the IRB at Washington University School of Medicine. Tissue Microarrays containing human non-neoplastic prostate specimens and prostatic adenocarcinomas with Gleason scores 5–9 were obtained from Biomax (Rockville, MD, USA).

Histology, Immunostaining, and Western blotting

Mouse tissues were fixed with 4% paraformaldehyde and embedded in paraffin. Sections of 7 μm were collected and stained with Hematoxylin and Eosin (H&E). Immunostaining was performed as described.[25] Briefly, deparaffinized sections were hydrated and antigen retrieval was done using citrate buffer (10mM, pH6), using a steamer. These slides were washed with 100mM glycine for 2×10′ and incubated with primary antibodies in humidified chamber overnight at 4°C. After washing with PBST 3×5′, samples were incubated with secondary antibodies for 1 hour at room temperature and washed with PBST 4×5′. After incubation with DAPI for 5′, the slides were washed again and mounted with Fluoromount G for imaging (Southern Biotech, Birmingham, AL, USA). Primary antibodies used were: from Abcam, Cambridge, UK: rabbit polyclonal Anti-ECadherin (ab53033 1:100), rabbit polyclonal anti-CK5 (ab24647, 1:100), mouse monoclonal anti-p63 (ab53039, 1:100), rabbit polyclonal anti-androgen receptor (ab47570, 1:100), rabbit polyclonal anti-SPP1 (ab8448, 1:100), mouse monoclonal anti-Synaptophysin (ab18008, 1:100), rabbit polyclonal anti-IL6 (ab6672, 1:200), rabbit polyclonal anti-c-MYC (ab39688, 1:100); from Life Technologies,

Carlsbad, CA, USA: rat monoclonal anti-CD44 (558739,1:100), mouse monoclonal anti-NFATc1 (556602, 1:100), Alexa Fluor 488 and 555-conjugated secondary antibodies (1:1000); from Cell Signaling Technologies, Danvers, MA, USA: rabbit polyclonal anti-Phospho STAT3 (9131, 1:100), rabbit monoclonal anti-STAT3 (4904, 1:50), rabbit monoclonal anti-pAKT (4060s, 1:100); from Sigma, St Louis, MO, USA: mouse monoclonal anti-αSMA (A2547, 1:100), HRP-conjugated secondary antibodies (1:1000); from Santa Cruz Technologies, Santa Cruz, CA, USA: rabbit polyclonal anti-IL1β (sc7884, 1:100), rabbit polyclonal anti-p21 (sc-471, 1:50); from Developmental Studies Hybridoma Bank, Iowa City, IA, USA: rat monoclonal anti-Cytokeratin 8 (TROMA-1, 1:100); from Bethyl Labs, Montgomery, TX, USA: rabbit monoclonal anti-PCNA (IHC-00012,1:100).

For Western blotting, protein extracts were separated by SDS–PAGE, transferred to Immobilon-P membranes (Millipore, Bedford, MA, USA) and probed by appropriate primary antibodies. After incubation with Alexa 680-conjugated goat anti-rabbit IgG (Life Technologies) and IRDye 800CW-conjugated goat anti-mouse IgG (Rockland, Gilbertsville, PA, USA) secondary antibodies, antibody complexes were visualized by an Odyssey Infrared Imaging System (LI-COR Biosciences, Lincoln, NE, USA).

RT-PCR

Total RNA was isolated using Trizol reagent (Life Technologies) and purified with an RNeasy Mini Kit (Qiagen, Valencia, CA, USA). cDNA was prepared by using the ThermoScript™ RT-PCR System (Life Technologies). PCR conditions were: 95°C, 4′, 35 × (94°C 35″; 55–59°C, 35″; 72°C, 35″). Primers used for 59°C annealing were: NFATc1-Fwd AAGAAGATGGTCCTGTCTGG and NFATc1-Rev GTAGTCTGGTACGTCGTAC; IL6-Fwd TGTGCAATGGCAATTCTGAT and IL6-Rev-GGTACTCCAGAAGACCAGAGGA; IL1β-Fwd CTGTGGCAGCTACCTGTGTC and ILβ-Rev TAATGGGAACGTCACACACC. Primers used for 58°C annealing were: Ccl3-Fwd CTGCCTGCTGCTTCTCCTAC and Ccl3-Rev CCCAGGTCTCTTTGGA-GTCA; IL1α-Fwd CAGTTCTGCCATTGACCATCT and IL1α-Rev CTCCTTGAAGGTGAAGTTGGA; Lcn2-Fwd AAACAGAAGGCAGCTTTACGA and Lcn2-Rev CCTGGAGCTTGGAACAAATG; Gapdh-Fwd CACTCTTCCACCTTCGATG and Gapdh-Rev TGCTGTAGCCGTATTCATTG. Primers used for 56°C annealing were: Saa3-F CCGTGAACTTCTGAACAGCCT and Saa3-R TGCCATCATTCTTTGCATCTTGA; Primers used for 55°C annealing were: Spp1-Fwd TGGTGCCTGACCCATCTCA and Spp1-Rev GTTTCTTGCTTAAAGTCATCCTTTTCTT.

Cell Culture

For primary tumor cell culture, prostates from *PCre/+;RT/+;TetO-NFATc1*^{Nuc} mice, treated for 14 week since P21, were harvested and cut into cubes <1mm^3 and cultured in DMEM-F12 (10% FBS, 5% penicillin/streptomycin and 2μg/ml Dox). Cells grew out of the tumor chunks were fed with fresh media every 2–3 days. A subculture with predominantly epithelial cells was established and expanded for subsequent experiments. RWPE-1, PC-3, LNCaP, and DU145 cells were originally obtained from the American Tissue Culture Collection (ATCC) and maintained according to ATCC guidelines. PC3, LNCaP, and DU145 cells were grown in RPMI media supplemented with 10% FBS. RWPE-1 cells were

maintained in Keratinocyte-SFM media supplemented with EGF and bovine pituitary extract.

Tumor graft in nude mice

For allografts, 3×10^6 aforementioned cultured tumor cells were injected subcutaneously into lower flanks of 16 male NCr nude mice (6 to 8-week-old, Taconic, Hudson, NY, USA). These mice were randomized into 4 groups. Group 1 was untreated and groups 2–4 were Dox-treated right after tumor cell injection. Group 2 was euthanized on the 70th day. Dox was stopped for group 3 on the 77th day and the mice were euthanized on the 84th day as tumors started to recede. Dox was stopped for group 4 on the 84th day and restarted on the 105th day. Group 4 was euthanized on the 126th day. Tumor volume was determined using a previously described formula.[45]

Castration

After anesthesia with 80mg/kg ketamine and 5mg/kg xylazine, each testis was gently pushed into the scrotum and surgically removed through a 0.5cm incision. The spermatic cord and vascular plexus were tied with sterile suture. Wound clips were used to close the incision and were removed 1 week after surgery.

Senescence Assay

Tissues sections were assessed for senescence by staining for SA-β-gal activity.[46] Briefly, prostate cryosections were fixed at room temperature for 3 minutes in 0.2% glutaraldehyde and 2% formaldehyde, rinsed with PBS, and incubated overnight at 37°C in SA-β-gal staining solution (40mM citric acid, 40mM H_2NaPO_4_$2H_2O$, 5mM $K_4Fe(CN)_6$_$3H_2O$, 5mM $K_3Fe(CN)_6$, 2mM $MgCl_2$, 150mM NaCl, pH6.0), containing 1mg/mL X-gal (U.S. Biochemical, Cleveland, OH, USA).

Acknowledgments

We thank Drs. Gerald Crabtree and Minggui Pan for providing the *TetO-NFATc1*^{Nuc} mice. F.C. is supported in part by grants from DoD (PC130118) and NIH (DK087960). Z.Y. is supported in part by NIH R01CA174714. L.D. is supported in part by grants from NIH (R01CA180006, R01CA178383, and U01HG006517).

References

1. Alberti C. Genetic and microenvironmental implications in prostate cancer progression and metastasis. Eur Rev Med Pharmacol Sci. 2008; 12:167–175. [PubMed: 18700688]
2. Graef IA, Chen F, Crabtree GR. NFAT signaling in vertebrate development. Curr Opin Genet Dev. 2001; 11:505–512. [PubMed: 11532391]
3. Pan MG, Xiong Y, Chen F. NFAT gene family in inflammation and cancer. Curr Mol Med. 2013; 13:543–554. [PubMed: 22950383]
4. Neal JW, Clipstone NA. A constitutively active NFATc1 mutant induces a transformed phenotype in 3T3-L1 fibroblasts. J Biol Chem. 2003; 278:17246–17254. [PubMed: 12598522]
5. Buchholz M, Schatz A, Wagner M, Michl P, Linhart T, Adler G, et al. Overexpression of c-myc in pancreatic cancer caused by ectopic activation of NFATc1 and the Ca2+/calcineurin signaling pathway. EMBO J. 2006; 25:3714–3724. [PubMed: 16874304]

6. Lehen'kyi V, Flourakis M, Skryma R, Prevarskaya N. TRPV6 channel controls prostate cancer cell proliferation via Ca(2+)/NFAT-dependent pathways. Oncogene. 2007; 26:7380–7385. [PubMed: 17533368]
7. Kawahara T, Kashiwagi E, Ide H, Li Y, Zheng Y, Ishiguro H, et al. The role of NFATc1 in prostate cancer progression: Cyclosporine A and tacrolimus inhibit cell proliferation, migration, and invasion. Prostate. 2015
8. Lee SJ, Lee K, Yang X, Jung C, Gardner T, Kim HS, et al. NFATc1 with AP-3 site binding specificity mediates gene expression of prostate-specific-membrane-antigen. J Mol Biol. 2003; 330:749–760. [PubMed: 12850144]
9. Rafiei S, Komarova SV. Molecular signaling pathways mediating osteoclastogenesis induced by prostate cancer cells. BMC Cancer. 2013; 13:605. [PubMed: 24370273]
10. Kavitha CV, Deep G, Gangar SC, Jain AK, Agarwal C, Agarwal R. Silibinin inhibits prostate cancer cells- and RANKL-induced osteoclastogenesis by targeting NFATc1, NF-kappaB, and AP-1 activation in RAW264. 7 cells. Mol Carcinog. 2014; 53:169–180. [PubMed: 23115104]
11. Jauliac S, Lopez-Rodriguez C, Shaw LM, Brown LF, Rao A, Toker A. The role of NFAT transcription factors in integrin-mediated carcinoma invasion. Nat Cell Biol. 2002; 4:540–544. [PubMed: 12080349]
12. Yoeli-Lerner M, Yiu GK, Rabinovitz I, Erhardt P, Jauliac S, Toker A. Akt blocks breast cancer cell motility and invasion through the transcription factor NFAT. Mol Cell. 2005; 20:539–550. [PubMed: 16307918]
13. Yiu GK, Toker A. NFAT induces breast cancer cell invasion by promoting the induction of cyclooxygenase-2. J Biol Chem. 2006; 281:12210–12217. [PubMed: 16505480]
14. Yiu GK, Kaunisto A, Chin YR, Toker A. NFAT promotes carcinoma invasive migration through glypican-6. Biochem J. 2011; 440:157–166. [PubMed: 21871017]
15. Foldynova-Trantirkova S, Sekyrova P, Tmejova K, Brumovska E, Bernatik O, Blankenfeldt W, et al. Breast cancer-specific mutations in CK1 epsilon inhibit Wnt/beta-catenin and activate the Wnt/Rac1/JNK and NFAT pathways to decrease cell adhesion and promote cell migration. Breast Cancer Res. 2010; 12:R30. [PubMed: 20507565]
16. Robbs BK, Cruz AL, Werneck MB, Mognol GP, Viola JP. Dual roles for NFAT transcription factor genes as oncogenes and tumor suppressors. Mol Cell Biol. 2008; 28:7168–7181. [PubMed: 18809576]
17. Wang Y, Jarad G, Tripathi P, Pan M, Cunningham J, Martin DR, et al. Activation of NFAT signaling in podocytes causes glomerulosclerosis. J Am Soc Nephrol. 2010; 21:1657–1666. [PubMed: 20651158]
18. Taylor BS, Schultz N, Hieronymus H, Gopalan A, Xiao Y, Carver BS, et al. Integrative genomic profiling of human prostate cancer. Cancer Cell. 2010; 18:11–22. [PubMed: 20579941]
19. Arredouani MS, Lu B, Bhasin M, Eljanne M, Yue W, Mosquera JM, et al. Identification of the transcription factor single-minded homologue 2 as a potential biomarker and immunotherapy target in prostate cancer. Clin Cancer Res. 2009; 15:5794–5802. [PubMed: 19737960]
20. Jiang J, Jia P, Zhao Z, Shen B. Key regulators in prostate cancer identified by co-expression module analysis. BMC Genomics. 2014; 15:1015. [PubMed: 25418933]
21. Wu X, Wu J, Huang J, Powell WC, Zhang J, Matusik RJ, et al. Generation of a prostate epithelial cell-specific Cre transgenic mouse model for tissue-specific gene ablation. Mech Dev. 2001; 101:61–69. [PubMed: 11231059]
22. Belteki G, Haigh J, Kabacs N, Haigh K, Sison K, Costantini F, et al. Conditional and inducible transgene expression in mice through the combinatorial use of Cre-mediated recombination and tetracycline induction. Nucleic Acids Res. 2005; 33:e51. [PubMed: 15784609]
23. Pan M, Winslow MM, Chen L, Kuo A, Felsher D, Crabtree GR. Enhanced NFATc1 Nuclear Occupancy Causes T Cell Activation Independent of CD28 Costimulation. J Immunol. 2007; 178:4315–4321. [PubMed: 17371988]
24. Lagunas L, Clipstone NA. Deregulated NFATc1 activity transforms murine fibroblasts via an autocrine growth factor-mediated Stat3-dependent pathway. J Cell Biochem. 2009; 108:237–248. [PubMed: 19565565]

25. Tripathi P, Wang Y, Coussens M, Manda KR, Casey AM, Lin C, et al. Activation of NFAT signaling establishes a tumorigenic microenvironment through cell autonomous and non-cell autonomous mechanisms. Oncogene. 2014; 33:1840–1849. [PubMed: 23624921]
26. Karlou M, Tzelepi V, Efstathiou E. Therapeutic targeting of the prostate cancer microenvironment. Nat Rev Urol. 2010; 7:494–509. [PubMed: 20818327]
27. Ding Z, Wu CJ, Chu GC, Xiao Y, Ho D, Zhang J, et al. SMAD4-dependent barrier constrains prostate cancer growth and metastatic progression. Nature. 2011; 470:269–273. [PubMed: 21289624]
28. Nilsson-Berglund LM, Zetterqvist AV, Nilsson-Ohman J, Sigvardsson M, Gonzalez Bosc LV, Smith ML, et al. Nuclear factor of activated T cells regulates osteopontin expression in arterial smooth muscle in response to diabetes-induced hyperglycemia. Arterioscler Thromb Vasc Biol. 2010; 30:218–224. [PubMed: 19965778]
29. Torti D, Trusolino L. Oncogene addiction as a foundational rationale for targeted anti-cancer therapy: promises and perils. EMBO Mol Med. 2011; 3:623–636. [PubMed: 21953712]
30. McCormick F. Cancer therapy based on oncogene addiction. J Surg Oncol. 2011; 103:464–467. [PubMed: 21480237]
31. Weinstein IB, Joe A. Oncogene addiction. Cancer Res. 2008; 68:3077–3080. discussion 3080. [PubMed: 18451130]
32. Suzman DL, Antonarakis ES. Castration-resistant prostate cancer: latest evidence and therapeutic implications. Ther Adv Med Oncol. 2014; 6:167–179. [PubMed: 25057303]
33. Carnero A, Paramio JM. The PTEN/PI3K/AKT Pathway in vivo, Cancer Mouse Models. Front Oncol. 2014; 4:252. [PubMed: 25295225]
34. Ortega-Molina A, Serrano M. PTEN in cancer, metabolism, and aging. Trends Endocrinol Metab. 2013; 24:184–189. [PubMed: 23245767]
35. Blagosklonny MV. Are p27 and p21 cytoplasmic oncoproteins? Cell Cycle. 2002; 1:391–393. [PubMed: 12548011]
36. Vincent AJ, Ren S, Harris LG, Devine DJ, Samant RS, Fodstad O, et al. Cytoplasmic translocation of p21 mediates NUPR1-induced chemoresistance: NUPR1 and p21 in chemoresistance. FEBS Lett. 2012; 586:3429–3434. [PubMed: 22858377]
37. Culig Z. Proinflammatory cytokine interleukin-6 in prostate carcinogenesis. Am J Clin Exp Urol. 2014; 2:231–238. [PubMed: 25374925]
38. Nguyen DP, Li J, Tewari AK. Inflammation and prostate cancer: the role of interleukin 6 (IL-6). BJU Int. 2014; 113:986–992. [PubMed: 24053309]
39. Zhao D, Pan C, Sun J, Gilbert C, Drews-Elger K, Azzam DJ, et al. VEGF drives cancer-initiating stem cells through VEGFR-2/Stat3 signaling to upregulate Myc and Sox2. Oncogene. 2014; 34:107–119.
40. Bowman T, Broome MA, Sinibaldi D, Wharton W, Pledger WJ, Sedivy JM, et al. Stat3-mediated Myc expression is required for Src transformation and PDGF-induced mitogenesis. Proc Natl Acad Sci U S A. 2001; 98:7319–7324. [PubMed: 11404481]
41. Kiuchi N, Nakajima K, Ichiba M, Fukada T, Narimatsu M, Mizuno K, et al. STAT3 is required for the gp130-mediated full activation of the c-myc gene. J Exp Med. 1999; 189:63–73. [PubMed: 9874564]
42. Phin S, Moore MW, Cotter PD. Genomic Rearrangements of PTEN in Prostate Cancer. Front Oncol. 2013; 3:240. [PubMed: 24062990]
43. Wei Z, Jiang X, Qiao H, Zhai B, Zhang L, Zhang Q, et al. STAT3 interacts with Skp2/p27/p21 pathway to regulate the motility and invasion of gastric cancer cells. Cell Signal. 2013; 25:931–938. [PubMed: 23333463]
44. Huang H, Zhao W, Yang D. Stat3 induces oncogenic Skp2 expression in human cervical carcinoma cells. Biochem Biophys Res Commun. 2012; 418:186–190. [PubMed: 22252296]
45. Janik P, Briand P, Hartmann NR. The effect of estrone-progesterone treatment on cell proliferation kinetics of hormone-dependent GR mouse mammary tumors. Cancer Res. 1975; 35:3698–3704. [PubMed: 1192428]
46. Zhang H, Teng Y, Kong Y, Kowalski PE, Cohen SN. Suppression of human tumor cell proliferation by Smurf2-induced senescence. J Cell Physiol. 2008; 215:613–620. [PubMed: 18181147]

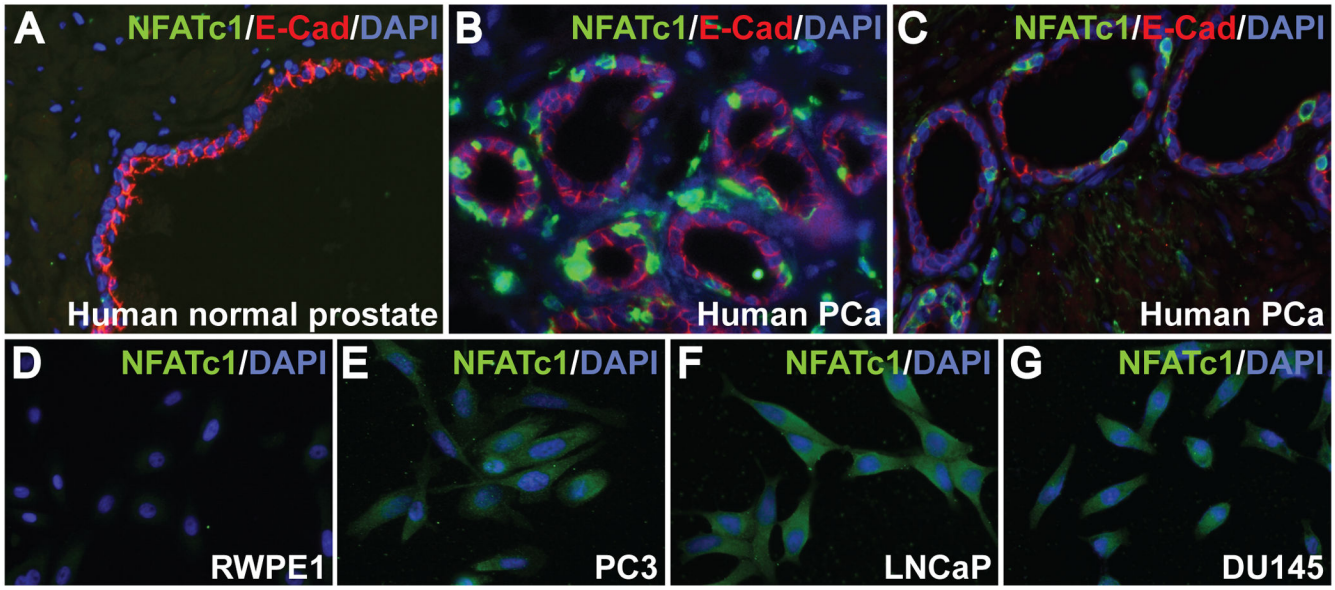

Figure 1. NFATc1 in human PCa and human PCa cell lines. NFATc1^{+} cells are absent in non-neoplastic human prostate

NFATc1^{+} cells are absent in non-neoplastic human prostate (**A**), but detected in human PCa (**B**–**C**). NFATc1 is expressed in the PCa cell lines but not in the non-tumorigenic RWPE1 cells (**D**–**G**).

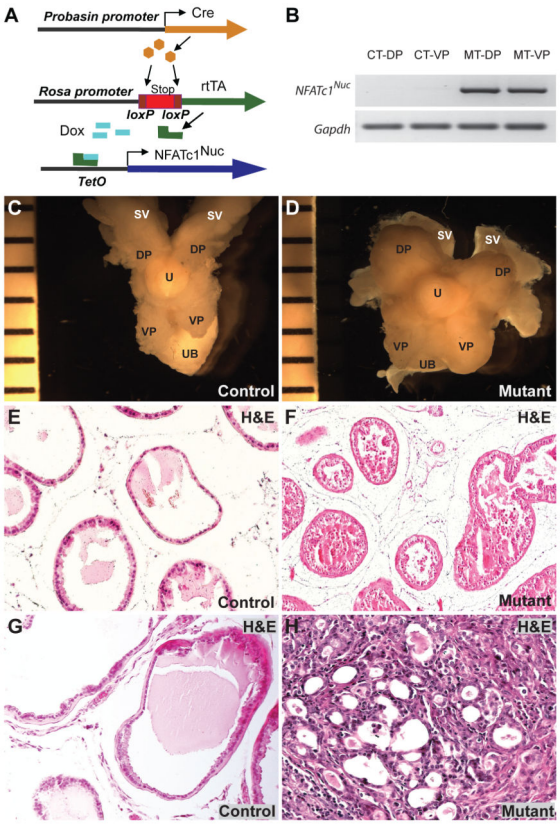

Figure 2. Inducible NFATc1 activation in prostatic epithelium causes PIN and prostatic adenocarcinoma

A, Cre induces the production of rtTA in prostatic epithelium. Binding of the Dox-rtTA complex to *TetO* leads to the production of NFATc1^{Nuc}. **B**, RT-PCR using RNA from prostates of control (CT) and mutant (MT) mice treated with Dox showed expression of NFATc1^{Nuc} only in the mutant prostates. DP: dorsal prostate. VP: ventral prostate. *TetO:* Tetracycline-responsive operator. *rtTA*: reverse tetracycline-controlled transactivator **C** and **D,** Prostates from control and mutant mice treated with Dox for 14 weeks starting from P21. U: Urethra; DP: Dorsal prostate; VP: Ventral prostate; UB: Urinary bladder. SV: Seminal vesicle. **E** and **F**, H&E Sections of the prostates from control and mutant mice treated with Dox for 6 weeks starting from P21. PINs are obvious in the mutants. **G** and **H,** Prostates from control and mutant treated with Dox for 14 weeks starting from P21.

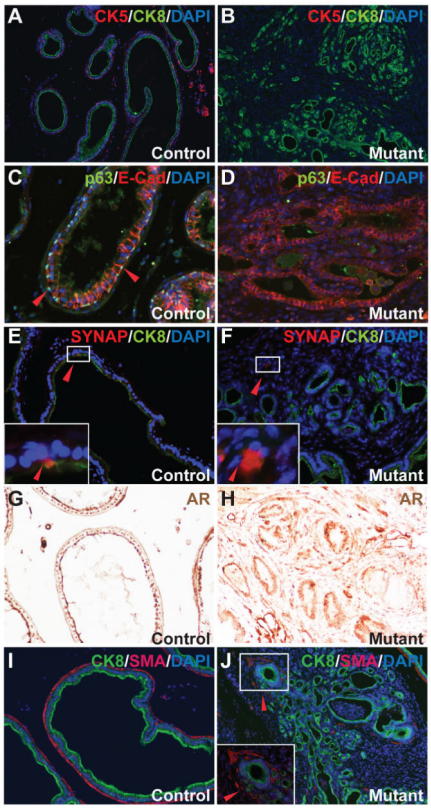

Figure 3. NFATc1-induced PCa has pathological changes resembling human PCa

Samples were from littermates treated with Dox from P21 for 14 weeks. **A,** the control prostatic gland has $CK5^+$ basal cells and $CK8^+$ luminal epithelium. **B**, the adenocarcinoma has predominantly $CK8^+$ luminal epithelial cells and few $CK5^+$ basal cells. **C**–**D**, p63+ basal cells were present in the control prostate (arrowheads) but absent from NFATc1-induced PCa. **E–F,** very few $SYNAP^+$ neuroendocrine cells are present in the periphery of the adenocarcinoma. **G** and **H,** mutant luminal epithelial cells retain nuclear AR expression. Unlike the control (**I**), discontinuation of the SMA^+ fibromuscular layer and invasion of the $CK8^+$ cells into the stroma (arrowheads in **J**) can be seen in the mutants.

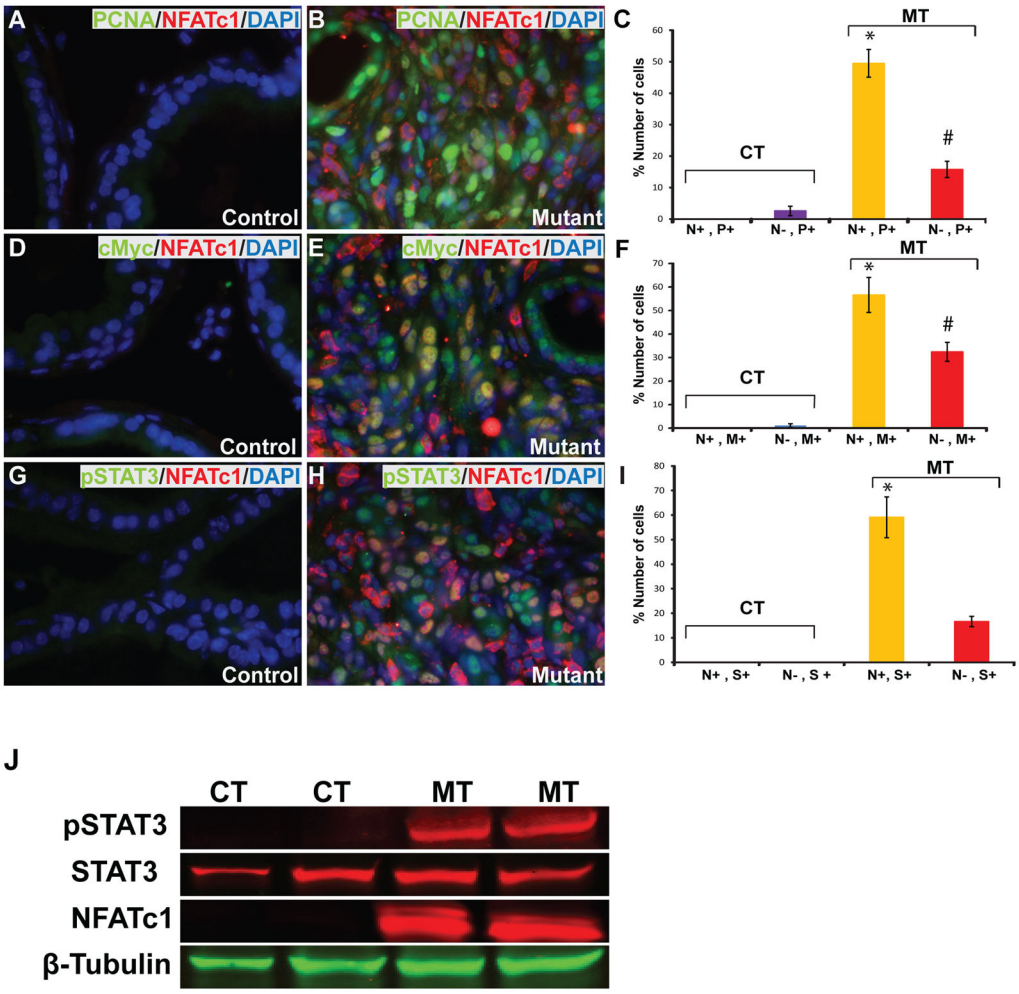

Figure 4. Active proliferation of NFATc1^{-} cells appears to result from a non-cell autonomous effects of NFATc1 activation in a promitogenic microenvironment

The prostate samples were from mice treated for 14 weeks from P21. N: NFATc1, P: PCNA, M: c-MYC, S: pSTAT3, CT: controls, MT: mutants. Immunostaining using NFATc1 and PCNA showed that a high percentage of NFATc1^{+} cells were actively proliferating (49.5±4.40%). The percentage of proliferating NFATc1^{-} cells in the mutants (15.8±2.57%), albeit smaller than that of the NFATc1^{+} cells in the mutants (*p <0.01, N=9), was still substantial and significantly more than the NFATc1^{-} cells in the controls (3.33±1.33% $^{\#}p$<0.01, N=9) (**A–C**). NFATc1 activation led to significant upregulation of c-MYC in the tumor tissue (**D–E**). 56.6±7.45% of NFATc1^{+} cells expressed c-MYC and a smaller percentage (32.4±4.0%) of NFATc1^{-} cells were c-MYC^{+} (*p<0.01, N=9). The NFATc1−, c-MYC+ cells are drastically more numerous in the mutants than in the controls (1.33±0.57%, $^{\#}p$<0.01, N=9) (**F**). Double immunostaining with antibodies against NFATc1 and phospho-STAT3 (pSTAT3-Tyr705) showed higher percentage of NFATc1^{+} cells with nuclear STAT3 (%) than NFATc1^{-} cells with nuclear STAT3 (17.67±1.45%, *p<0.01, N=9) (**G–I**). However, the percentage of NFATc1−, pSTAT3+ cells is much higher in the mutants than in the control prostates (0%, N=9). Western blot analysis of prostate lysates from controls and PCa from mutants was probed by antibodies against STAT3 (revealing total

STAT3 levels) and pSTAT3 (revealing the levels of activated STAT3). The results showed activation of STAT3 specifically in NFATc1-induced PCa, while the levels of total STAT3 were unchanged (**J**). All data are presented as mean ± s.d and two-tailed t-tests were performed between groups.

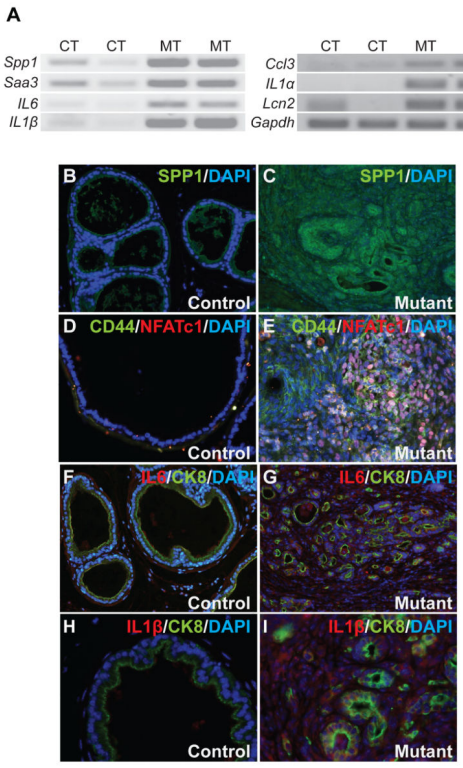

Figure 5. Increased expression of a number of secreted factors in NFATc1-induced PCa

A. Number of secretory factors known to play in PCa progression like SPP1, IL6, IL1β, IL1α, along with several other genes were evaluated for transcriptional changes with RT-PCR using RNA from prostates of control (CT) and mutant (MT) mice treated with Dox for 14 weeks. **B–I,** Immunostaining showed more extensive expression of Spp1, CD44, IL6, and IL1β in PCa from the prostates of mutant mice compared to their littermate controls.

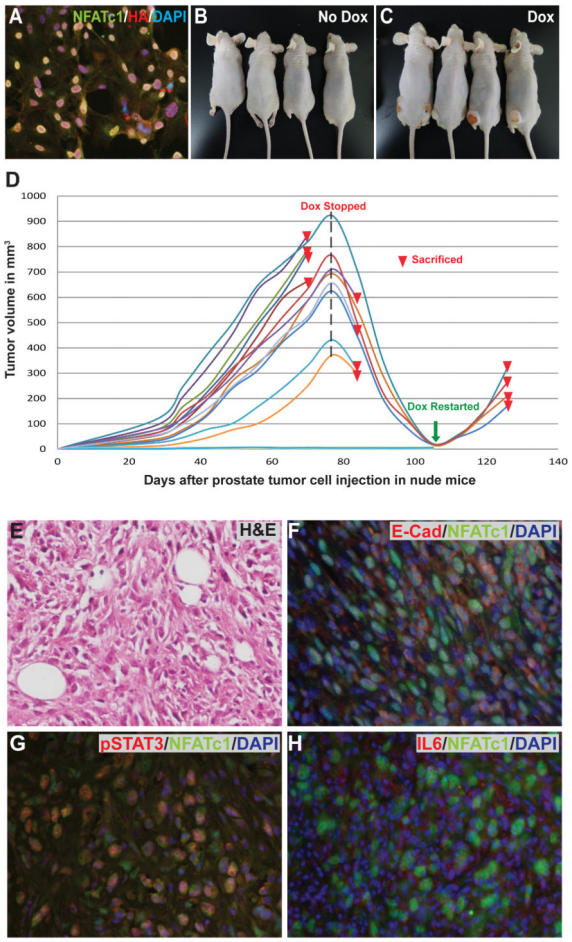

Figure 6. Allografts of NFATc1-induced tumors showed continuous dependency on NFATc1 for tumor progression and survival but not on T cell functions

Cells from NFATc1-induced PCa samples were isolated and cultured. Most of the cultured cells expressed NFATc1 and the HA tag (**A**). Cultured tumor cells were injected subcutaneously into the lower flanks of nude mice. 100% of the Dox-treated recipients developed tumors by 4 weeks, whereas none of the untreated mice did (**B–D**). Termination of Dox treatment resulted in significant decrease in tumor size. Such decrease was reverted if Dox treatment was restarted (**D**). Representative images of H&E stained nude mice allograft (**E**). The allograft tumors predominantly consist of NFATc1^{+} cells expressing E-Cad (**F**). Similar to the original tumor, extensive pSTAT3 (**G**) and IL6 (**H**) expression was observed in the allograft tumors.

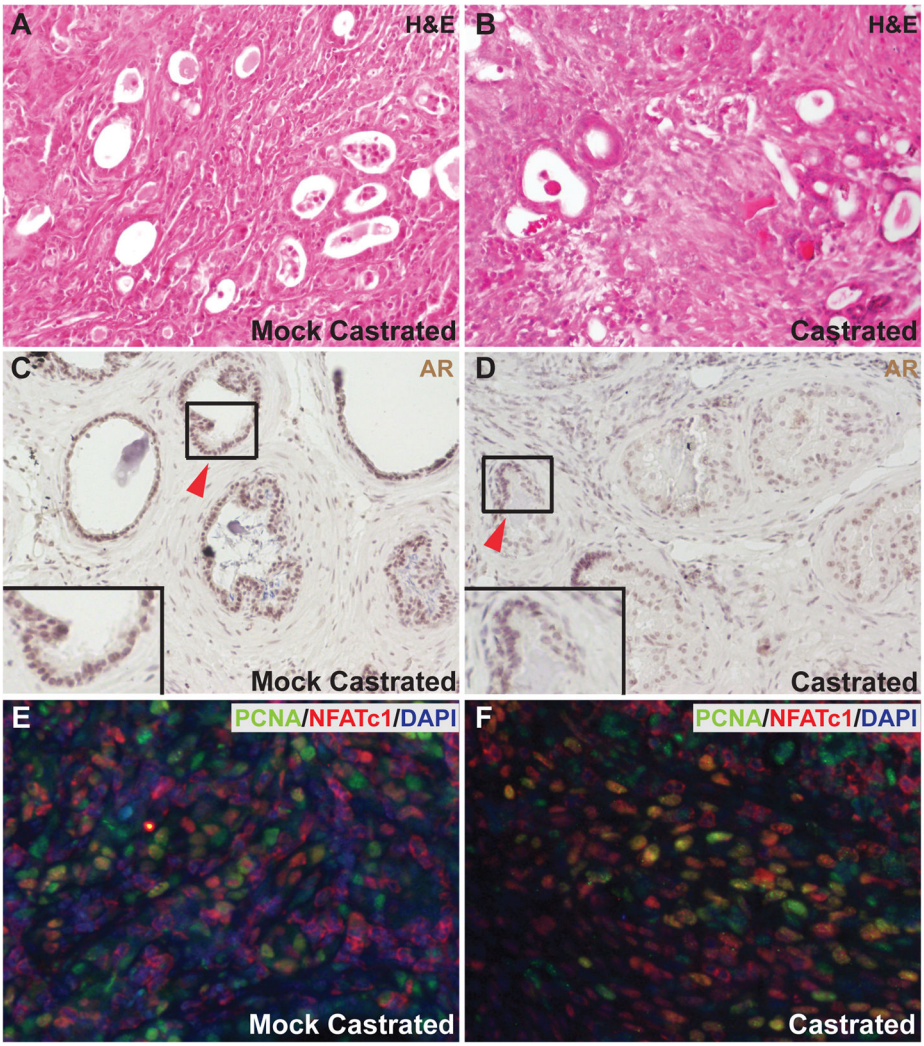

Figure 7. NFATc1-induced tumors are castration resistant

Representative images of H&E stained sections of tumors from mock-castrated and castrated mice showing PCa (**A–B**). Predominantly nuclear AR is present in mock-castrated mice. AR signal is weak and diffuse in the sample from the castrated mutants. The insets represent higher magnification images of the black rectangles indicated by arrows (**C–D**). The numbers of proliferating cells in mock-castrated and castrated mice expressing NFATc1 and PCNA markers (**E–F**) are very similar.

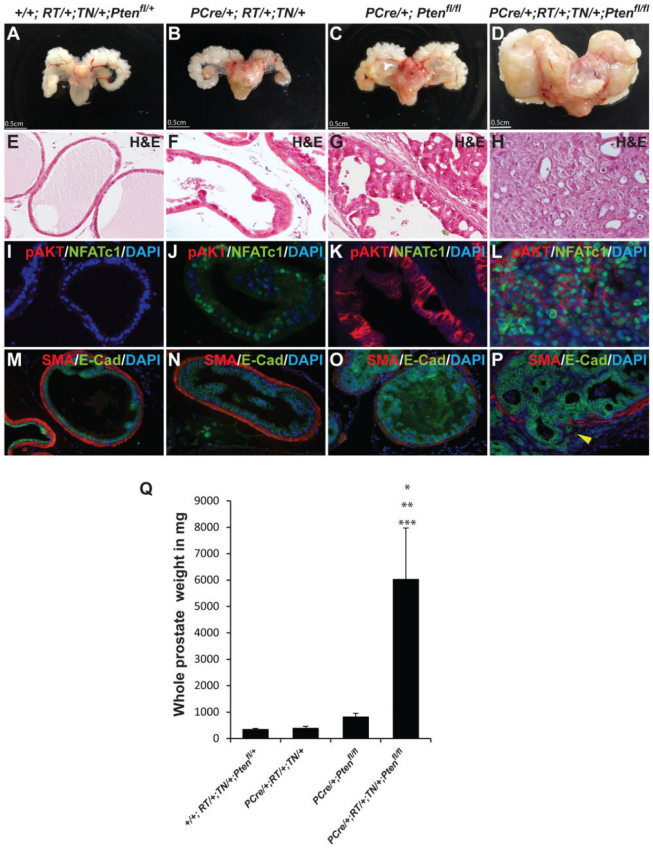

Figure 8. NFATc1 and PI3K-Akt signaling pathway synergize to drive accelerated tumor formation

Representative images of tumors with *PCre/+;RT/+;TN/+;Pten*$^{fl/fl}$ double mutants showing significantly enlarged tumors compared to control (no NFATc1 activation or *Pten* deletion), *PCre/+;RT/+;TN/+* (NFATc1 activation alone), and *PCre/+;Pten*$^{fl/fl}$ (*Pten* deletion alone) groups (**A–D**). H&E staining of prostates at 10 weeks of age reveals normal glands in controls, PIN in *PCre/+;RT/+;TN/+* mice, morphologically more advanced PIN in *PCre/+;Pten*$^{fl/fl}$ mice, and advanced PCa in *PCre/+;RT/+;TN/+;Pten*$^{fl/fl}$ double mutant mice (**E–H**). Deletion of Pten results in activation of AKT in *PCre/+;Pten*$^{fl/fl}$ and *PCre/+;RT/+;TN/+;Pten*$^{fl/fl}$ mutant mice whereas no significant levels of pAKT were detected in control and NFATc1 activation only groups (**I–L**). Discontinuation of the SMA^{+} fibromuscular layer and invasion of the E-Cad^{+} cells into the stroma (arrowhead in **P**) can be seen in the mutants (**M–P**). Average whole prostate weight of the *PCre/+;RT/+;TN/+;Pten*$^{fl/fl}$ mice is drastically higher than those of the *+/+;RT/+;TN/+;Pten*$^{fl/+}$ mice (*$p < 0.05$, N=7) *PCre/+;RT/+;TN/+ mice* (**$p < 0.05$, N=7), and *PCre/+;Pten*$^{fl/fl}$ mice (***$p < 0.05$, N=7). (**Q**). All data are presented as mean ± s.d. Two- tailed t-tests were performed for comparison between groups.

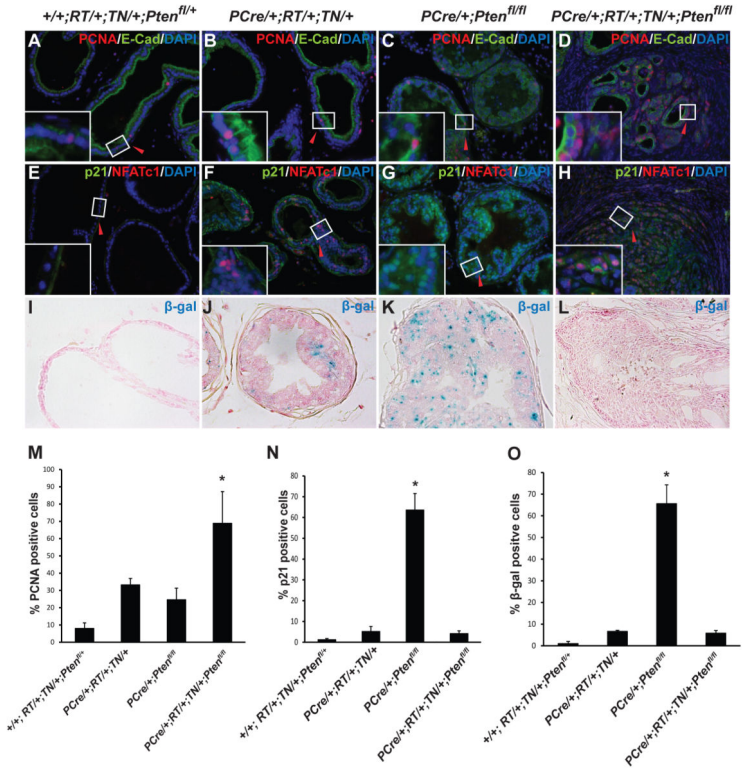

Figure 9. NFAT Activation overcomes PTEN-loss-induced cellular senescence in PCa

PCre/+;RT/+;TN/+;Pten$^{fl/fl}$ mutant prostates have a much larger number of proliferating E-Cad^{+} cells when compared to control, *PCre/+;RT/+;TN/+*, and *PCre/+;Pten*$^{fl/fl}$ mice (**A**–**D**). The insets are higher magnification images of the white rectangles indicated by arrows. Quantification of PCNA staining of 10-week-old prostates is shown in **M**. Asterisk indicates statistical significance between *PCre/+;RT/+;TN/+;Pten*$^{fl/fl}$ double mutants and *PCre/+;Pten*$^{fl/fl}$ single mutants (*p <0.05, N=5). **E–L:** Senescence analysis of prostates through p21 and SA-β-gal staining. Control and *PCre/+;RT/+;TN/+* mutant lack p21-expressing cells. Mostly nuclear p21 expression was seen in large numbers of prostate epithelial cells in the *PCre/+;Pten*$^{fl/fl}$ mice, whereas such cells are essentially absent in the *PCre/+;RT/+;TN/+;Pten*$^{fl/fl}$ double mutants (*p <0.05, N=5) (**E–H, N**). The insets represent higher magnification images of the white rectangles indicated by arrows. Quantification of p21^{+} cells in 10-week-old prostates is shown in (**N**). **I–L:** Senescence-associated β-gal staining of prostates from 10-week-old mice. Prostates from control and *PCre/+;RT/+;TN/+* mice had very few senescent cells. Prostates of the *PCre/+;Pten*$^{fl/fl}$ mice contain a large number of senescent cells, when compared to prostates of the *PCre/+;RT/+;TN/+;Pten*$^{fl/fl}$ double mutants showing drastically fewer p21^{+} senescent cells (*p <0.05, N=5) (**I–L, O**). Quantification of SA-β-gal^{+} cells in 10-week-old prostates (**O)** is consistent with the p21 data. Prostates from control and *PCre/+;RT/+;TN/+* mice had few SA-β-gal^{+} senescent cells. Prostates of the *PCre/+;Pten*$^{fl/fl}$ mice contain a large number of SA-β-gal^{+} senescent cells, when compared to prostates of the *PCre/+;RT/+;TN/+;Pten*$^{fl/fl}$ double mutants that had significantly fewer SA-β-gal^{+} senescent cells (*p <0.05, N=5). All data are presented as mean ± s.d. Two- tailed t-tests were performed for comparison between groups. Asterisk

indicates statistical significance between the *PCre/+;Pten*$^{fl/fl}$ single mutants and the *PCre/+;RT/+;TN/+;Pten*$^{fl/fl}$ double mutants.